

This result may be due to the difference in angular momentum of the two compound nuclei. More definite evidence on this point could be obtained from similar studies of (α, xn) and (He^3, xn) reactions that involved the same compound nucleus, rather than the same target. Such experiments are currently in progress in our laboratory.

The angular distribution of the (He^3, n) reaction product has been compared in a qualitative way with the distorted-wave theory. The results are sufficiently encouraging to merit both a more complete calculation,

in which account is taken of all the levels populated by the stripping reaction, as well as experiments with far more detailed angular resolution.

ACKNOWLEDGMENTS

The cooperation of M. Oselka and the operating crew of the Argonne National Laboratory 60-in. cyclotron is gratefully acknowledged. The distorted-wave calculations were kindly performed by Dr. R. L. Hahn and Dr. R. Drisko at Oak Ridge National Laboratory with a code prepared by Dr. R. Drisko.

Nuclear Structure of Na²². V. Doppler-Shift Attenuation Measurements*

P. PAUL,† J. W. OLNES, AND E. K. WARBURTON

Brookhaven National Laboratory, Upton, New York

(Received 10 May 1968)

The mean lifetimes of seven nuclear levels of Na²² have been measured by the Doppler-shift attenuation method. The F¹⁹(α, n)Na²² reaction was used to populate the levels. γ rays were observed at 0° to the α beam with a Ge(Li) detector. The results, when averaged with previous work, yield the following mean lives (in psec) for the indicated levels: 0.891 (12.25±1.75), 1.528 (3.5±0.6), 1.984 (1.74±0.34), 2.211 (20₋₈⁺²⁵), 2.572 (5.7±0.9), 2.969 (0.060±0.013), and 3.059 (0.040±0.01), where the levels are designated by their excitation energies (in MeV). For the five lowest levels the lifetimes were obtained from an analysis of Doppler-shifted line shapes; the remaining two lifetimes were determined from conventional centroid-shift analysis. The latter method also gave a lifetime of 5.2±0.9 psec for the 1.346-MeV level of F¹⁹. Some information was obtained on the $M2/E1$ mixing ratios of the ground-state and first-excited-state transitions from the $J^\pi=2^-$ 2.572-MeV level of Na²². Evidence for a $K=1$ odd-parity rotational band in Na²² is discussed.

I. INTRODUCTION

MEASUREMENTS have been reported in previous publications^{1,2} from this laboratory which gave lifetime determinations for several bound states in Na²² below 3.1 MeV and upper and/or lower limits for several others. Figure 1 shows the levels¹⁻⁶ of Na²² which are pertinent to this work. Mean lifetimes of 3.8±0.9 and 1.60±0.34 psec were obtained for the 1.528- and 1.984-MeV levels. For the levels at 0.891, 2.211, and 2.572 MeV lower limits of the order of 10 psec had been obtained, whereas for the doublet levels at 2.97 and 3.06 MeV upper limits of 0.14 and 0.09

psec, respectively, were given. Since then, various measurements on some of the longer-lived states have been made, all using the centroid-shift version of the Doppler-shift attenuation technique. Blaugrund *et al.*⁷ used a gaseous stopper to obtain lifetimes of 10.8±1.8, 12±2, and 4.5±1.0 psec for the states at 0.891, 2.211, and 2.572 MeV. Pronko *et al.*⁸ gave $\tau=3.9_{-1.0}^{+2.2}$ and 11.1_{-3.7}^{+11.2} psec for the states at 1.528 and 0.891 MeV while Kavanagh⁹ obtained 3.2±1.0 and 18±7 psec for these same states.

Lifetimes of 10 psec or longer press the centroid-shift version of the Doppler-shift attenuation method to the limits of solid stopping materials. Also, the use of gaseous stoppers has not yet been studied extensively and is subject to some systematic errors that are hard to assess.¹⁰ Thus, a reexamination of the long lifetimes

* Work performed under the auspices of the U. S. Atomic Energy Commission.

† A. P. Sloan fellow, guest physicist from State University of New York at Stony Brook, New York.

¹ E. K. Warburton, J. W. Olnes, and A. R. Poletti, Phys. Rev. **160**, 938 (1967).

² A. R. Poletti, E. K. Warburton, J. W. Olnes, and S. Hechtl, Phys. Rev. **162**, 1040 (1967).

³ A. R. Poletti, E. K. Warburton, and J. W. Olnes, Phys. Rev. **164**, 1379 (1967).

⁴ E. K. Warburton, A. R. Poletti, and J. W. Olnes, Phys. Rev. **168**, 1232 (1968).

⁵ T. Wei, Bull. Am. Phys. Soc. **13**, 85 (1968); (private communication).

⁶ R. Haight (private communication).

⁷ A. E. Blaugrund, A. Fisher, and A. Schwarzschild, Nucl. Phys. **A107**, 411 (1968).

⁸ J. G. Pronko, C. Rolfs, and H. J. Maier, Phys. Rev. **167**, 1066 (1968).

⁹ R. W. Kavanagh, Bull. Am. Phys. Soc. **12**, 913 (1967).

¹⁰ Two possible systematic errors are (1) uncertainty in the "density" effect, i.e., that effect which makes a dilute gas about 10% more effective in stopping charged particles than the same material in the solid state and (2) local heating of the gas by the beam with an associated decrease in the effective gas density.

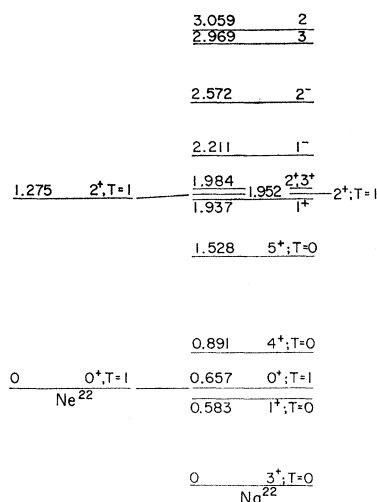


FIG. 1. The low-lying levels of Na²² and Ne²². The figure is from Ref. 4 with additional information on the 1.952- and 2.572-MeV levels provided by the Na²³(*d,t*)Na²² angular distribution results of Wei (Ref. 5) and the Na²³(*p,d*)Na²² angular distribution results of Haight (Ref. 6).

by use of another version of the Doppler-shift method seemed desirable. The present investigation uses the detailed analysis of the attenuated Doppler line shape¹ to reexamine all the long-lived states in a consistent way. The long lifetimes are obtained relative to the lifetime of the 1.528-MeV state, which is reasonably well known and lies in a range where the centroid version of the Doppler-shift method is still quite accurate. It will be shown that the relative lifetimes so obtained are quite insensitive to uncertainties in the nuclear stopping for our experimental conditions.

In addition, values are presented for the short lifetimes of the doublet levels at 2.969 and 3.059 MeV in Na²² obtained in a conventional centroid-shift analysis.

Finally, as a by-product, information about multipole-mixing ratios for γ ray decay of the state at 2.572 MeV has been obtained from angular distributions of some de-excitation γ rays.

II. DETERMINATION OF THE LONG LIFETIMES

The mean lives of the states in Na²² at 0.891, 1.528, 1.984, 2.211, and 2.572 MeV are all known to be in the range 1–50 psec. They were thus all investigated with a technique selected for its relative sensitivity to long lifetimes. This technique involves the measurement of the attenuated Doppler line shape and a detailed fit to it with a known recoil ion slowing-down function. All aspects of this method have been described in detail previously¹ and the present experimental setup and analysis are essentially identical to those of this previous work.

The F¹⁹(α,n)Na²² reaction ($Q = -1.949$ MeV) was

used to populate each of the states at an energy as close to each threshold as possible consistent with adequate yield. Specifically, the bombarding energies of 4.7, 4.7, 5.5, 5.5, and 6.1 MeV obtained with the doubly ionized He⁴ beam of the Brookhaven National Laboratory Van de Graaff accelerator, correspond to the above sequence of five levels from 0.891 to 2.572 MeV. The kinematics of the reaction is then such that the excited Na²² nuclei recoil into a narrow forward cone, where they are slowed down in a solid stopping material (see Appendix A of Ref. 1). To be suitable for the measurement of psec lifetimes, the stopping material itself must have a stopping-time constant α of comparable size. This requires low density and if possible large Z . Backings of CaF₂ ($\rho = 3.18$ g/cm³), SrF₂ ($\rho = 4.24$ g/cm³), and metallic Li⁶ ($\rho = 0.45$ g/cm³) were used. The first two had the advantage that the target material (F¹⁹) is imbedded in the backing so that no correction had to be made for the time the recoiling ion spends in the target. The Li backing provides the solid stopper with the lowest density and results in a stopping-time constant $\alpha = 2.1$ psec for the pure metal. The isotope Li⁶ was used rather than natural Li in order to eliminate the very strong 482-keV γ ray from inelastic scattering on Li⁷. In this case, the target was a 100- μ g/cm²-thick layer of CaF₂. Target and backing were produced in a two-step evaporation: a 1-mg/cm²-thick layer of Li⁶ was evaporated onto a copper foil, and was then covered by the layer of CaF₂. Targets were transferred from the evaporator into the target chamber under an argon atmosphere without visible signs of oxidation. Actual lifetime measurements showed, however, that the backing had apparently not remained completely metallic. This will be discussed later.

The γ rays from the de-excitation of Na²² were detected at 0° relative to the incident beam in a 2-cm³ Ge(Li) detector which had an intrinsic resolution of about 2.3 keV for the Co⁶⁰ lines. The spectra were recorded in a 1024-channel pulse-height analyzer. Care was taken during runs to hold the count rate at a low level so that no discernible pileup effects were produced on the line shapes of standard γ -ray source peaks. Part of a typical γ -ray spectrum obtained in this way with the Li⁶-backed CaF₂ target is shown in Fig. 2. The nucleus, as well as the initial and final state for each transition, is indicated for each peak. These peaks are the full-energy components of each γ ray. The features on which the analysis is based, can be seen best in the transitions from the 1.528- and 1.984-MeV states. A sharp peak of a width given by the intrinsic counter resolution arises from those γ rays which were emitted after the recoiling ion had come to rest in the backing. A tail or broad peak on the high-energy side of the “stopped” peak results from the Doppler-shifted γ rays emitted during recoil at decreasing velocities. The ratio of the areas under the “stopped” and “fast” peaks is roughly proportional to

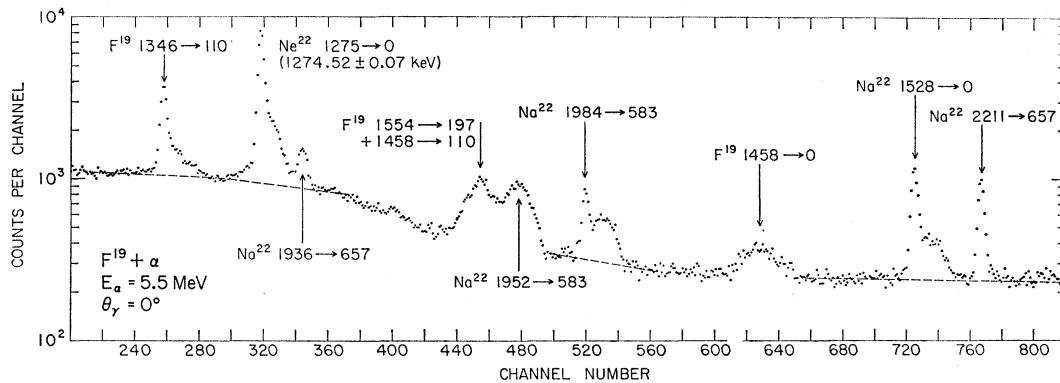


FIG. 2. Portion of a 1024-channel γ -ray spectrum from bombardment of a $100\text{-}\mu\text{g}/\text{cm}^2$ CaF_2 target with 5.5-MeV α particles observed at 0° with a 2-cc Ge(Li) detector. The target backing was Li^6 metal (see text). The energy dispersion is 0.624 keV/channel and the detector resolution is ~ 2.5 -keV FWHM. Full-energy-loss peaks corresponding to γ -ray transitions in F^{19} , Ne^{22} , and Na^{22} are identified by the energies (in keV) of the initial and final states between which the transitions take place. The dashed curves are backgrounds assumed in the line-shape analysis discussed in the text.

the lifetime of the excited state.¹¹ It is thus immediately obvious that the lifetimes of the 1.984- and 1.528-MeV states are shorter than that of the 2.211-MeV level. In general, of course, the recoil distribution, due to the angular distribution of the associated particle emitted in the reaction, will generate a complex γ -ray line shape even for the case of recoil into vacuum. It has been shown that even in that case a line-shape analysis can extract the lifetime of the state involved with great accuracy.¹² With the present kinematics and geometry, however, the energy of the associated particle is small enough so that line-shape effects are induced essentially only by the recoil velocity attenuation. Thus one measurement at 0° suffices to determine the lifetime of the state. This is not necessarily true for some of the parasitic peaks that are observed in the spectrum of Fig. 2, such as the peak due to the Ne^{22} γ ray. The $\text{F}^{19}(\alpha, p)\text{Ne}^{22}$ reaction populating this state is exothermic, and the clearly visible tail on the low-energy side of this peak arises from nuclei that recoil into the backward hemisphere, thus recoiling into vacuum. Our analysis fails for this peak. On the other hand, the F^{19} state is populated in an endothermic reaction, but not close to threshold. This line shape therefore contains angular distribution effects, as well as the attenuated recoil effect. However, the lifetime can still be extracted with reasonable accuracy through determination of the centroid shift. The ratio F between attenuated and vacuum Doppler shift in this case can again be obtained from one measurement alone, if the energy scale in the spectrum is known with sufficient precision. In the present case all the unshifted γ -ray energies have previously been measured¹ with high accuracy. Then F is given by $F = (E_\gamma - E_{\gamma 0})/\Delta E_{\text{vac}}$, where E_γ and $E_{\gamma 0}$ are the centroid energy and the energy

of the stopped peak, respectively. The full Doppler shift ΔE_{vac} can be calculated with sufficient accuracy assuming an isotropic distribution of the associated particle, and can be checked by determining the energy difference between the high-energy cutoff of the "fast" component and the "stopped" peak. The position of the latter is always obtained from a Gaussian fit to the peak.

Detailed line-shape fits were made to all Na^{22} peaks with a long lifetime. This procedure again is explained in detail in Ref. 1, and we will repeat here only the main points. A least-squares fit was performed on a computer to the line-shape distribution. The slowing-down function was represented by the equation,

$$-M_1 \frac{dv_z}{dt} = K_n \left(\frac{v_z}{v_0} \right)^{-1} + K_e \left(\frac{v_z}{v_0} \right), \quad (1)$$

where K_n represents the so-called nuclear contribution, and K_e the electronic contribution. These two terms suffice for the low initial recoil velocities created in the present reaction. A fit to the line-shape distribution as a function of v_z involves the variation of two parameters, namely $\gamma_i^2 = (K_e/K_n)v_i^2$ and $x = \alpha/\tau$ where $\alpha = M_i v_0 / K_e \rho$ is the electronic stopping time. K_n and K_e may be obtained from the sources listed in Ref. 1 with guidance from the theories of Lindhard, Scharff, and Schiøtt,¹³ and Lindhard and Scharff,¹⁴ respectively. Actually, some experimental information about the values of both constants has been assembled in previous lifetime studies by the Brookhaven group.¹ This experience shows that in the case of a unique initial velocity, good and meaningful line-shape fits are obtained by simulating the sum of the effects of the nuclear stopping and the large-angle scattering by a $1/v$ dependence as

¹¹ J. W. Olness and E. K. Warburton, Phys. Rev. **151**, 792 (1966).

¹² T. R. Fisher, S. S. Hanna, D. C. Healey, and P. Paul, Phys. Rev. (to be published).

¹³ J. Lindhard, M. Scharff, and H. E. Schiøtt, Kgl. Danske Videnskab. Selskab, Mat. Fys. Medd. **33**, No. 14 (1963).

¹⁴ J. Lindhard and M. Scharff, Phys. Rev. **124**, 128 (1961).

TABLE I. Stopping parameters for different backing materials.

Stopping material	CaF ₂	SrF ₂	Li ⁶ (expected)	Li ⁶ (measured)	Li ⁶ O
α (psec)	0.69±0.10	0.75±0.11	2.14±0.32	1.37±0.3	0.59±0.09
K_n/K_e	0.14±0.05 ^a	0.13±0.05	0.082 ^b	0.09±0.03 ^c	0.094 ^b

^a Average of present determination with that of Ref. 1.

^b From Lindhard-Scharff-Schiøtt theory (see Appendix B of Ref. 1).

^c Assumed.

in Eq. (1), and by treating K_n as an empirical parameter. Results obtained by this procedure agree with those obtained with explicit treatment of the large-angle scattering.¹⁵ Our analysis may fail, however, in the case of line shapes containing a large initial velocity distribution.

Best values of K_n/K_e (or γ_i^2) are usually achieved when K_n is close to the value obtained from nuclear stopping theory without scattering.^{1,13} K_n does not enter very critically into the line-shape fit because the nuclear stopping has its largest effect at low velocities very near the "stopped peak." In the following, the

results of this procedure, applied to the various states, will be discussed.

1.528-MeV Level

Attenuated Doppler line shapes obtained for the 1.528-MeV γ ray with the three different backings are shown in Fig. 3. The stopping time constant α is given for each backing in Table I. The ratio R of "stopped" to "fast" component of the line indicated in Fig. 3 can be seen to decrease as the value of α increases, as expected. Least-squares fits have been made to these line shapes (solid curves). The values of K_n/K_e , assumed for each backing, are listed in Table I. The lifetimes, obtained with these parameters from the data with CaF₂ and SrF₂ backings, are collected in Table II where they are compared to results given previously. The uncertainties associated with the present values of τ include the uncertainties of the analysis as well as in the parameters K_n and K_e . A comparison shows that all values of τ agree within the quoted errors. It is interesting to note that the error of the line-shape analysis is generally smaller than that of the centroid determination. This reflects the fact that the line shape contains more detailed information than the centroid. The weighted averaged value, $\tau=3.5\pm0.6$ psec, will now be used as a standard against which the other lifetimes are calibrated.

The expected value of α (= 2.14 psec) for the metallic Li⁶ backing is such that the most precise result for τ should result from the use of this backing; however, the data obtained with this backing could not be used without precaution. The value of α depends directly on the density of the backing, which in the case of Li

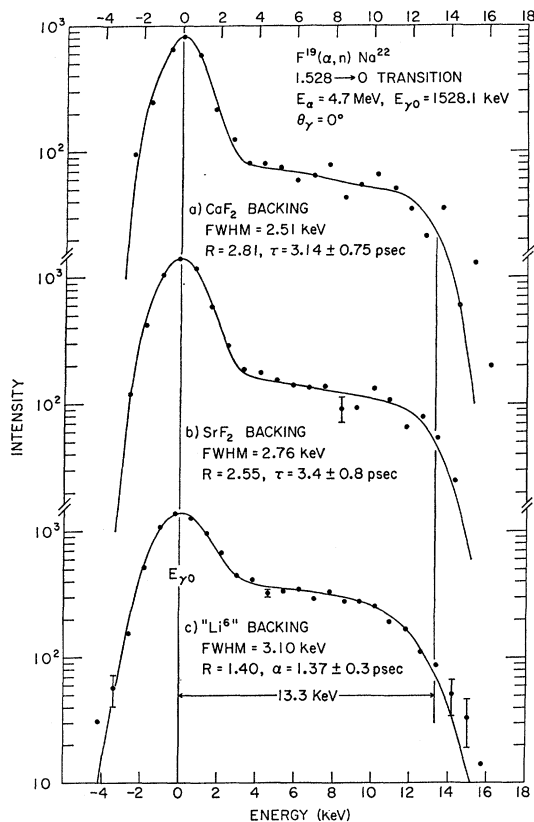


FIG. 3. The full-energy-loss peak of the 1.528-MeV γ ray corresponding to the Na²² 1.528 \rightarrow 0 transition observed at 0° to the beam. The γ ray results from direct feeding of the 1.528-MeV level in the F¹⁹(α, n)Na²² reaction initiated in the indicated targets. Background has been subtracted. The solid curves are theoretical fits to the line shapes as described in the text. R is the ratio of the "stopped" and "fast" components of the line.

¹⁵ A. E. Blaugrund, Nucl. Phys. 88, 501 (1966).

TABLE II. Resumé of lifetime measurements for the Na²² 1.528-MeV level.

Method	τ (psec)	Reference	Stopping material
D. S. line shape	3.4 ± 0.8	this work	SrF ₂
D. S. line shape	3.14 ^{-0.78} +0.62	this work	CaF ₂
D. S. centroid	3.2 ± 1.0	Kavanagh ^a	Xenon gas
D. S. centroid	3.9 ^{-1.0} +2.2	Pronko <i>et al</i> ^b	CaF ₂
D. S. line shape	3.8 ± 0.9	Warburton <i>et al</i> . ^c	CaF ₂
Average	3.5 ± 0.6		

^a Reference 9.

^b Reference 8.

^c Reference 1.

increases two or threefold if a layer of appreciable thickness (i.e., on the order of the distance traveled by the Na^{22} ions in the mean life) of the metal is oxidized, or otherwise chemically altered. We have therefore rather derived the effective value of α from the 1.528-MeV line shape and the established lifetime of the state. Assuming that the ratio K_n/K_e is the same as for the metal (this was checked by a calculation to hold within 10% for all feasible chemical compounds of Li^6), the line shape of the Li^6 run shown in Fig. 3 yields $\alpha = 1.37 \pm 0.3$ psec with K_n/K_e as listed in Table I. Table I shows that this value of α is smaller than that expected for the pure metal, but not reduced to the fully-oxidized case. In the following, this effective α is used to obtain lifetimes of other states from line shapes obtained with the " Li^6 " backing. In this, and all other fits, to the " Li^6 " data a correction was made for the finite CaF_2 target thickness. That is, the stopping function used was that for a combination of two stopping materials.

2.572-MeV Level

The lifetime of this state is now obtained relative to that of the 1.528-MeV level measured in the same target and backing. Line shapes observed for the 2.57-MeV γ ray are shown in part (a) and (b) of Fig. 4. The CaF_2 -backed run yields a ratio $x(2.57)/x(1.53) = 0.50 \pm 0.05$, where $x = \alpha/\tau$, which leads to $\tau(2.57) = 7.1 \pm 1.4$ psec. It turns out that this ratio is remarkably insensitive to the parameter γ_i^2 that contains the "nuclear stopping" effects. Thus there was no evidence for any systematic change of the best-fitting values of either $x(2.57)/x(1.53)$ or $x(1.98)/x(1.53)$, as γ_i^2 was varied over a region a factor of 3 each side of the best-fitting value of ~ 20 . Indeed, the statistically

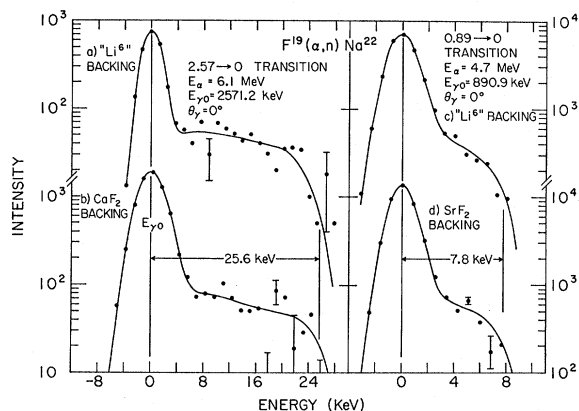


FIG. 4. The full-energy-loss peaks of the 2.572- and 0.891-MeV γ rays corresponding to the Na^{22} 2.572 \rightarrow 0 and 0.891 \rightarrow 0 transitions observed at 0° to the beam. The γ rays result from direct feeding of the two levels in the $\text{F}^{19}(\alpha, n)\text{Na}^{22}$ reaction initiated in the indicated targets. Background has been subtracted. The solid curves are theoretical fits to the line shapes as explained in the text.

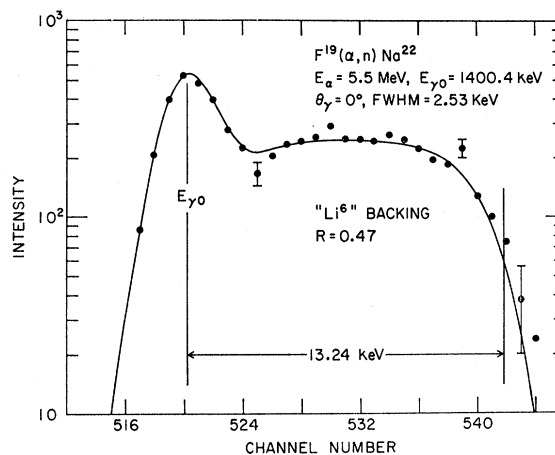


FIG. 5. The full-energy-loss peak of the 1400-keV γ ray from the Na^{22} 1.98 \rightarrow 0.58 transition observed at 0° to the beam. The γ ray results from direct feeding of the Na^{22} 1.984-MeV level in the $\text{F}^{19}(\alpha, n)\text{Na}^{22}$ reaction initiated in a " Li^6 " backed CaF_2 target. Background has been subtracted. The solid curve is a theoretical fit to the γ -ray line shape as explained in the text. R is the resulting ratio of the "stopped" and "fast" components of the line.

more accurate ratio, $x(1.984)/x(1.528)$, was constant to 3% over this range of γ_i^2 .

By comparison to the 1.528-MeV result, the " Li^6 "-backed run shown in Fig. 4 yields $\tau(2.57) = 6.0 \pm 1.6$ psec. The average for the two backings is $\tau = 6.5 \pm 1.2$ psec, which is somewhat faster than the limit of > 10 psec given previously^{1,16} and in fair agreement with the value of 4.5 ± 1.0 psec obtained by Blaugrund *et al.*⁷ We adopt as the average of all available results $\tau(2.57) = 5.7 \pm 0.9$ psec.

1.984-MeV Level

The lifetime of this level is obtained from analysis of the 1.40-MeV γ ray resulting from the 1.98 \rightarrow 0.58 transition. A value of 1.6 ± 0.34 psec had been obtained previously¹ with a CaF_2 backing. Thus the " Li^6 " backing should produce a particularly large tail on the γ -ray line and this is shown in Figs. 2 and 5. We therefore analyze the data as another check on the " Li^6 " backing. The ratio of "stopped" to "fast" component is here reduced to 0.47. One now also observes a slight dip in the line shape at low velocities. The theoretical fit drawn in Fig. 5 gives the first indication that the procedure we use to account for the large-angle scattering may be inadequate since it cannot reproduce this dip, although the discrepancy is perhaps not statistically significant. The fit yields $x(1.40)/x(1.53) = 1.87 \pm 0.10$ or $\tau(1.98) = 1.87 \pm 0.35$ psec, in agreement with the value of 1.60 ± 0.34 psec obtained¹ from the CaF_2 backing. The average value thus is $\tau(1.98) = 1.74 \pm 0.34$ psec.

¹⁶ The previous lower limit of 10 psec for the 2.572-MeV level (Ref. 1) was in error by a factor of 2; it should have been 5 psec. In addition, experience gained in the present work has taught us that the lower limits given in Ref. 1 are too optimistic by a factor of up to 2.

TABLE III. Mean lives of the 0.891- and 2.211-MeV levels.

Reference	τ (psec)		Stopper
	0.891-MeV level	2.211-MeV level	
This work	13.4 \pm 3.0	20 ₋₈ ⁺²⁵	solid
Kavanagh ^a	18.0 \pm 7.0		gas
Blaugrund <i>et al.</i> ^b	10.8 \pm 1.8	12 \pm 2	gas
Pronko <i>et al.</i> ^c	11.1 _{-3,7} ^{+11,2}		solid
Average:	12.25 \pm 1.75		

^a Reference 9.
^b Reference 7.
^c Reference 8.

0.891- and 2.211-MeV Levels

According to previous results,⁷ these two states have lifetimes greater than 10 psec. Thus the "Li⁶"-backed runs should give the best results. Parts (c) and (d) of Fig. 4 show the shapes observed for the 0.891-keV line. The "Li⁶"-backed run yields a ratio $x(0.89)/x(1.53) = 0.26 \pm 0.04$ or $\tau(0.89) = 13.4 \pm 3.0$ psec. This agrees with results obtained using the other backings and the previous limit.¹ Table III compares the present results with other published values. Averaging the four values gives $\tau(0.89) = 12.25 \pm 1.75$ psec. This takes all quoted errors at face value although our estimate of the *inherent* errors of Doppler-shift measurements is considerably greater than that of Blaugrund *et al.*⁷

Just from a comparison of the tails, it is obvious that the 2.211-MeV state has an even longer lifetime. The "Li⁶"-backed run yields $\tau(2.21) = 20_{-8}^{+25}$ psec. This lifetime represents the limit of what can reasonably be measured with our "Li⁶" backing. Blaugrund *et al.*⁷ obtained 12 ± 2 psec with a gas stopper.

F¹⁹ 1.346-MeV Level

The 1.236-MeV γ ray shown in Fig. 2 shows a definite Doppler line shape. A mere visual comparison of the size of the tail on this line and that for the 1.528-MeV γ ray (Fig. 3) and the 0.891-MeV γ ray (Fig. 4) indicates a mean life of between 3 and 10 psec for the level in F¹⁹. As we pointed out before, the kinematics of the reaction for this level are such that the effects on the line shape due to the recoil of the associated particle may not be negligible. Instead of a line-shape analysis we, therefore, use only the centroid information. For the data of Fig. 2, the difference in the positions of the centroid of the "stopped" peak and the centroid of the entire distribution is $\Delta E = 3.05 \pm 0.20$ channels or 1.90 ± 0.12 keV. This leads to $F = 0.160 \pm 0.024$ where the full Doppler shift of 11.7 ± 1.6 keV was calculated assuming the F¹⁹(α, α')F¹⁹ angular distribution may be characterized by $\langle \cos \theta_{c.m.} \rangle = 0.0 \pm 0.33$ at $E_\alpha = 5.5$ MeV. The mean life was deduced from this F value by numerical integration¹ using $\alpha = 1.20 \pm 0.26$ psec and the Lindhard-Scharff-Schiøtt value for K_n .^{1,18} The

electronic stopping time α was obtained by extrapolation¹ from the value given previously for Na²² ions. This procedure yields $\tau = 4.8 \pm 1.3$ psec. A similar analysis of the data obtained using a SrF₂ target yielded $\tau = 5.4 \pm 1.0$ psec. The weighted average of these two determinations is $\tau(\text{F}^{19} \text{ 1.35-MeV level}) = 5.2 \pm 0.9$ psec.

III. LIFETIMES OF THE 2.97- AND 3.06-MeV STATES

Previous measurements¹ of these mean lifetimes have established upper limits of < 0.14 psec for the 2.97-MeV level, and < 0.09 psec for the 3.06-MeV level. Determination of such short lifetimes requires a technique different from the one used in Sec. II. Although line-shape analysis procedures have been used very successfully for lifetimes down into the 10-fsec range, and indeed may be most precise at these limits, they require a very careful and tedious study.¹² It was felt that a sufficiently reliable measurement (i.e., within the errors of the stopping function) could be obtained in these cases from an analysis of the centroid shift alone. Specifically the difference between the full ("vacuum") and the attenuated Doppler shift have been measured at 0°. The two states were populated using, again, the F¹⁹(α, n)Na²² reaction in which the Na²² ions emerge into a forward cone.

The centroid position of the full Doppler shift was determined with a SF₆ gas target, the attenuated centroid position with a SrF₂ target thick enough (~ 1 mg/cm²) so that the target material was also the stopping material for the Na²² recoil nuclei. With this choice of targets and backing, all target-thickness corrections are negligible. Since the difference between full and attenuated centroid position is small, care was exercised to remove all sources of possible systematic errors. γ rays were detected at 0° relative to the incident α beam in the 2-cm³ Ge(Li) detector placed at a distance of 6 cm from the target cell. Effects on the measured line energies due to finite detector solid angle or possible alignment error are wholly negligible. The α beam entered the target cell through a 0.03-mil Ni window, and was stopped at the far wall on a Ta foil. The procedure was then as follows. For the measurement of the full shift, the chamber was filled with SF₆ to a pressure of 60 Torr (~ 1 mg/cm²). Then the gas was pumped out and a solid 1-mg/cm² SrF₂ target was lowered into the beam, this being the only change in the experimental conditions.

The measurements were carried out at an incident He⁴⁺⁺ beam energy of 7.29 MeV. A loss of ~ 230 keV in the Ni window resulted in an incident energy of 7.06 MeV. Both the gas and solid targets were about 340 keV thick and thus the actual mean bombarding energy was about 6.9 MeV in both measurements. The comparison consisted of three sets of measurements, gas target-solid target-gas target, each for a period of ~ 5 h for a net accumulated charge each of 700 μC .

Counting rates during all three runs were about equal, and low enough so that no pileup effect could be detected on standard source lines in the γ -ray spectra. The spectrum was stored in a 1024-channel pulse-height analyzer with standard reference lines provided at the lower end of the spectrum by a Mn^{54} source (834.95 ± 0.04 keV) and at the upper end (1195 keV) by a precision pulser. The Na^{22} $0.891 \rightarrow 0$ transition (890.87 ± 0.20 keV) provided an additional energy standard. In order to monitor against gain shifts, the data were read out at 1-h intervals; whatever gain shift was present was later removed by a computation which matched the standard peaks of the short runs.

The pertinent data are shown in Fig. 6, which contains the sum of all spectra for the solid and gas target measurements. It is evident from the centroid positions indicated in Fig. 6 that the Doppler shift in the solid SrF_2 target is less than that in the gaseous SF_6 target for both the $3.06 \rightarrow 1.95$ and $2.97 \rightarrow 1.95$ transitions. The difference is, respectively, 1.45 ± 0.25 channels (0.66 ± 0.11 keV) and 1.85 ± 0.25 channels (0.84 ± 0.11 keV). The full Doppler shifts determined from the centroids observed in SF_6 gas and the previously¹ determined values of $E_{\gamma 0}$ are 13.2 and 11.7 keV, respectively, with an error of ± 1 keV. These compare to values calculated from the kinematics, assuming an isotropic distribution of the associated neutron and a mean α energy of 6.9 MeV, of 11.8 and 10.9 keV, again with an uncertainty of ± 1 keV. In computing $F(\tau)$ we have used the average values of 12.5 and 11.3 keV, respectively, together with the difference between the gas- and solid-target shifts to yield the following values for the attenuation factors in SrF_2 : $F = 0.950 \pm 0.009$ for the $3.06 \rightarrow 1.95$ transition, and $F = 0.926 \pm 0.012$ for the $2.97 \rightarrow 1.95$ transition. The corresponding values for the mean lives of the initial states based on $\alpha = 0.75 \pm 0.11$ psec for SrF_2 are $\tau(3.06) = 0.04 \pm 0.01$ psec and $\tau(2.97) = 0.060 \pm 0.013$ psec.

Various backgrounds were assumed in analyzing the peaks of Fig. 6; exponential, straight line, and Gaussian, in order to investigate the extent to which the computed centroids may have been influenced by the particular form assumed. The results indicate that the background subtraction introduces an uncertainty of about ± 0.25 channels which is responsible for the assigned errors above. The line shapes of the transition peaks were found to be very similar for the gas and the solid targets, as one expects, for the case where F is not far from unity. One possible source of error arises in the gas-target runs from target material that might be adsorbed on either the entrance foil or the beam stopper. A check run with the pumped-out cell proved that such adsorption was negligible.

IV. ANGULAR DISTRIBUTION MEASUREMENTS

The level at 2.57 MeV is the only one for which the present results add new information on spin and parity.

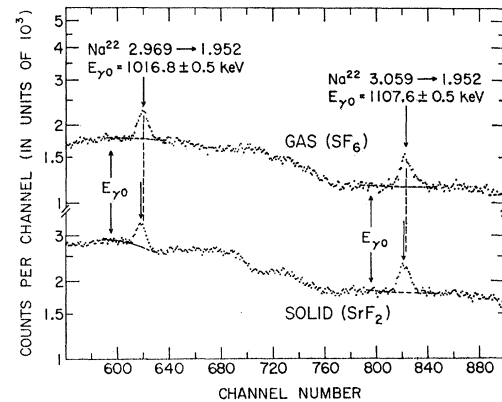


Fig. 6. Partial γ -ray spectra showing the full-energy-loss peaks corresponding to the Na^{22} $2.97 \rightarrow 1.95$ and $3.06 \rightarrow 1.95$ transitions initiated in gas and solid targets. The spectra were observed at 0° to the beam. Both γ -ray peaks are Doppler shifted as can be seen by the indicated centroids of the four peaks and the indicated γ -ray rest energies ($E_{\gamma 0}$). The differences between the Doppler shifts observed in the gas and solid targets can be inferred from the figure.

The lifetime of the state precludes transitions of multipolarity greater than quadrupole, and in view of the observed transitions to the ground state and 0.58-MeV level, restrict the spin of the level to 1, 2, or 3.² Previous angular correlation measurements² allow $J=1$ or 2. The mean life of $\tau = 5.7 \pm 0.9$ psec gives a width for the $81 \pm 3\%$ ground-state branch of $\Gamma_{\gamma 0} = (0.94 \pm 0.15) \times 10^{-4}$ eV. This width corresponds to $E2$ and $M2$ transition strengths of 0.28 ± 0.04 and 7.1 ± 1.1 Weisskopf units,¹⁷ respectively. No $M2$ transition with such a large strength¹⁸ is known, and since this multipole strength in the present case is expected to be reduced by the isospin selection rule,¹⁸ $M2$ character and thus negative parity can be ruled out with confidence if the 2.57-MeV state has $J=1$. The pickup reactions $\text{Na}^{22}(p,d)\text{Na}^{22}$ and $\text{Na}^{22}(d,t)\text{Na}^{22}$ to this state in Na^{22} have recently been studied by Wei⁵ and Haight.⁶ A DWBA analysis indicates in both cases pickup of a p -wave nucleon, thus implying $J^\pi = 1^-$, or 2^- for the final state. Since a 1^- assignment is eliminated by the argument given above, the spin and parity of the 2.57-MeV state must be $J^\pi = 2^-$.

In addition to these lifetime measurements, a precise remeasurement of angular distributions of γ rays originating from this level was undertaken with the hope of directly discriminating between the possibilities $J=1$ and $J=2$. The 2.57-MeV level was formed by the $\text{F}^{19}(\alpha,n)\text{Na}^{22}$ reaction at a bombarding energy of 6.1 MeV. Previous work had already shown that the transition to the 0.58-MeV state may exhibit a large anisotropy, whereas the ground-state transition was

¹⁷ D. H. Wilkinson, in *Nuclear Spectroscopy*, edited by F. Ajzenberg-Selove (Academic Press Inc., New York, 1960), part B, p. 862 ff.

¹⁸ E. K. Warburton, in *Isobaric Spin in Nuclear Physics*, edited by J. D. Fox and D. Robson (Academic Press Inc., New York, 1966), pp. 90-112.

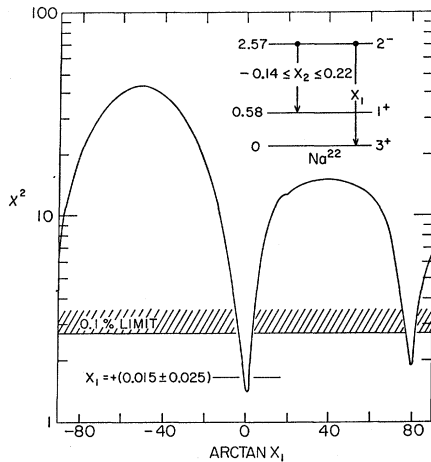


FIG. 7. χ^2 versus $\arctan x$ from simultaneous analysis of the Na^{22} $2.57 \rightarrow 0$ and $2.57 \rightarrow 0.58$ γ -ray angular distributions. The data analyzed includes that of Ref. 2 (see Table III and Fig. 4 of Ref. 2) as well as that obtained in the present work (see text). χ^2 , representing the goodness of fit to the experimental data, is shown as a function of $\arctan x_1$, where x_1 is the $M2/E1$ mixing ratio of the $2.57 \rightarrow 0$ transition. The mixing ratio x_2 of the $2.57 \rightarrow 0.58$ transition has been restricted to lie within the region allowed by the 0.1% limit of Ref. 2. The resulting limitations on x_1 are indicated. A similar analysis for x_2 gives the limitations quoted in the text.

found to be nearly isotropic. Both angular distributions were therefore remeasured with sufficient statistics and care in the alignment of the setup to guarantee an accuracy of $\pm 2\%$ at each angle. An 8-cc Ge(Li) detector was used in this measurement. The $0.58 \rightarrow 0$ transition observed in the same reaction must be completely isotropic because of total deorientation of the initial state in the Ni target backing before decay. Its measured distribution thus provided a satisfactory internal check on the alignment of the apparatus.

Least-squares fits to the full-energy peaks of the $2.57 \rightarrow 0$ and $2.57 \rightarrow 0.58$ transitions observed at $\theta = 0^\circ, 30^\circ, 45^\circ, 60^\circ,$ and 90° gave the following coefficients in a Legendre polynomial expansion: $2.57 \rightarrow 0.58$; $a_2 = -(0.44 \pm 0.04)$, $a_4 = +(0.097 \pm 0.051)$; and $2.57 \rightarrow 0$; $a_2 = -(0.097 \pm 0.015)$, $a_4 = -(0.016 \pm 0.017)$. Analyses of these coefficients in terms of initial and final spins must include multipole mixing ratios for both transitions, since the lifetime of the 2.57-MeV state indicates that either can contain some contribution from $M2$. With two mixing ratios $x_1(2.57 \rightarrow 0)$ and $x_2(2.57 \rightarrow 0.58)$ as variables, the Legendre coefficients listed above could be reproduced for either $J=1$ or 2 with plausible values for x_1 and x_2 . Thus, the angular distributions do not discriminate between these two spins; however, they establish limits for x_1 and x_2 if $J=2$ is assumed. The method used to obtain limits on x_1 is illustrated in Fig. 7, which shows a conventional χ^2 -versus- x_1 plot, resulting from combining a plot of this type obtained from the present angular-distribution data with one obtained² previously at this laboratory. This analysis gives $x_1 = +(0.015 \pm 0.025)$

and $x_2 = +(0.00 \pm 0.1)$, i.e., both mixing ratios are consistent with pure $E1$ radiation. The larger $M2/E1$ mixing ratios, previously allowed² for the $2.57 \rightarrow 0$ and $2.57 \rightarrow 0.58$ transitions, are ruled out from the observed lifetime in the same manner as for a pure $M2$ assignment to the $2.57 \rightarrow 0$ transition. For the $2.57 \rightarrow 0$ transition, we can give a limit on the $M2$ strength by combining the 0.1% confidence limit on x_1^2 with the ground-state radiative width. This results in a limit on the $M2$ strength of < 0.05 Wu.

V. DISCUSSION

The levels of established positive parity in Na^{22} up to the excitation energy shown in Fig. 1 can be ascribed to a series of rotational bands with remarkable success. This aspect has been discussed elsewhere⁴ and the modifications to the lifetimes of the positive-parity states, from the work reviewed or presented here, do not alter this description: the lowest is the ground-state band with $K=3, T=0$, and the spin sequence $3^+, 4^+, 5^+ \dots$; the next higher band has $K=0, T=0$ with $J=1^+, 3^+ \dots$; finally, we have a $K=0, T=1$ band beginning with the $J=0^+, 2^+$ levels at 0.657 and 1.952 MeV. These bands are predicted by either the Nilsson model or the SU_3 model.¹⁹ The only positive-parity state not contained in this band sequence is the 1^+ state at 1.937 MeV.²⁰

The present work adds new and interesting information on the negative-parity states at 2.211 and 2.572 MeV. Their spin sequence $1^-, 2^-$ suggests the possibility of a negative-parity band with $K=1, T=0$; the next member possibly being the $J=3$ state at 2.969 MeV whose parity, however, has not yet been established, or the 3.53-MeV level for which $J \geq 2$ is all that is known. In the following we discuss the properties of these states in the light of this speculation.

For easier comparison, some pertinent decay properties are collected in Table IV. In this table, final states are grouped according to the suggested band structure outlined above. Members of a negative-parity band could be expected to show similarities in their decay to the other bands. Since at most two transitions to lower states have been observed so far for each negative-parity state, this discussion can only check for inconsistencies rather than agreement. It can, however, suggest future work.

From Table IV we first note that the $E1$ transitions are strongly inhibited. The average strength of $\Delta T=0$ $E1$ transitions in light self-conjugate nuclei is $\sim 10^{-8}$ Wu¹⁷ while the $\Delta T=0$ $E1$ transitions of Table IV have a typical strength of $\sim 10^{-5}$ – 10^{-6} . Even more startling is the small strength of the allowed ($\Delta T=1$) $E1$ transitions. The average strength of allowed $E1$ transitions

¹⁹ M. Harvey (private communication).

²⁰ It is tempting to conjecture that the 1.937-MeV level is the intrinsic state of a $K=1$ positive-parity band with the 3.059-MeV level being the second member of this band.

TABLE IV. Comparison of decay properties of the Na²² states at 2.211, 2.572, and 2.969 MeV. Final states are grouped according to bands as discussed in the text. *E1*, *M1*, and *M2* multipoles are considered. Transition strengths (in Wu) are based on the lifetime measurements reviewed or presented in the text and on the branching ratios of Warburton *et al.*^a The last rows give upper limits on possible transitions within a negative-parity band. The theoretical *M1* estimates are based on an assumed value of $|g_K - g_R| = 0.034$ as discussed in the text.

Final state		Initial state (MeV)		
<i>E_x</i> (MeV)	<i>J^π</i> ; <i>T, K</i>	2.211 (<i>J^π</i> = 1 ⁻) ^b	2.572 (<i>J^π</i> = 2 ⁻)	2.969 (<i>J</i> = 3)
0	3 ⁺	0.05 ± 0.05 (<i>M2</i>)	1.0 × 10 ⁻⁶ (<i>E1</i>) ^c , < 0.05 (<i>M2</i>) ^c	< 7.9 × 10 ⁻⁶ (<i>E1</i>)
0.891	4 ⁺	...	< 1.46 (<i>M2</i>)	< 2.2 × 10 ⁻⁶ (<i>E1</i>)
0.583	1 ⁺	< 4.3 × 10 ⁻⁷ (<i>E1</i>)	5.2 × 10 ⁻⁶ (<i>E1</i>) ^c	< 12 (<i>M2</i>)
1.984	(3 ⁺)	...	< 4.3 × 10 ⁻⁶ (<i>E1</i>)	< 1.3 × 10 ⁻³ (<i>E1</i>)
0.657	0 ⁺	1.6 × 10 ⁻⁶ (<i>E1</i>)	< 1.9 (<i>M2</i>)	...
1.952	2 ⁺	...	< 3.6 × 10 ⁻⁶ (<i>E1</i>)	2.0 × 10 ⁻² (<i>E1</i>)
2.211	1 ⁻	...	{ expt: < 8.1 × 10 ⁻³ (<i>M1</i>)	...
2.572	2 ⁻	...	{ theo: 4.6 × 10 ⁻⁶ (<i>M1</i>)	{ expt: < 1.66 (<i>M1</i>)
			...	{ theo: 5.9 × 10 ⁻⁶ (<i>M1</i>)

^a Reference 1.

^b The lifetime used for the 2.211-MeV level is 20 psec.

^c These values make use of the multipole ratios presented in this work.

is ~ 0.055 Wu,¹⁷ while the 1⁻ and 2⁻ levels decay with $\Delta T=1$ *E1* strengths no greater than 2×10^{-5} Wu. Thus, the weakness of these *E1* rates suggests a basic selection rule. Such a selection rule, for instance, is provided by the *SU*₃ model. On this model, the three positive-parity bands belong to the symmetry group (82), while the odd-parity band belongs to the group (82) if it arises from $p^{-1}(2s, 1d)^7$, and (90) if it arises from $(2s, 1d)^5(2p, 1f)$. Neither of these latter groups can be connected to (82) by an *E1* or *M2* transition and thus both *E1* and *M2* transitions are forbidden in the *SU*₃ model.¹⁹ Thus we have a qualitative explanation for the weakness of the *E1* transitions, which in turn adds credence to our suggestion of an odd-parity band. There is, however, a discrepancy between the suggested inclusion of the 2.97-MeV level in the odd-parity band and this selection rule. The $\Delta T=1$ 2.97 → 1.95 transition has a strength of 0.02 Wu if it is *E1* and this is $\sim 10^3$ times stronger than the $\Delta T=1$ decays of the 1⁻ and 2⁻ levels. A determination of the parity of the 2.97-MeV level and the properties of the 3.53-MeV level²¹ is of first importance for testing the rotational model of Na²². Other tests of the model proposed for the odd-

parity levels would be provided by a search for weak transitions connecting the odd- and even-parity levels. The transitions, which are both interesting and capable of being observed without undue experimental improvements on previous work, can be inferred from Table IV. In particular, it appears worthwhile to confirm or disprove the uncertain (1 ± 1%) 2.21 → 0 branch, since a 1% branch corresponds to a rather strong transition for an *M2* transition that is inhibited by both isospin¹⁸ and *SU*₃ selection rules.

The experimental limits and theoretical predictions for intra-band *M1* transitions given at the bottom of Table IV are included to show that the absence of such intra-band transitions is as expected. It is seen that the observation of intra-band transitions between the odd-parity states would be quite difficult. The theoretical predictions for these *M1* rates (the *E2* contributions are expected to be negligible) were made using the value of $(g_K - g_R) = 0.034$ inferred⁴ from the intra-band *M1* rates connecting the positive-parity levels.

ACKNOWLEDGMENTS

We would like to thank C. Z. Nawrocki and F. A. Mahnken for their advice and enthusiastic participation in the preparation of the various solid targets used in this work. Thanks are also due to T. Wei and R. Haight who sent us details of their work prior to publication.

²¹ It was previously suggested that the 3.53-MeV level was the 5⁺ *T*=0 level of the *K*=0, *T*=0 band (Refs. 3 and 4). However, the fact that the γ -ray angular distributions obtained for the decay of this level (Ref. 2) are inconsistent with such an assignment was overlooked. For a 5⁺ assignment the mean γ -decay mode would be, from the results of Ref. 2, 3.53 → 1.98 → 0.58; this would be a 5⁺ → 3⁺ → 1⁺ sequence with two essentially pure *E2* transitions requiring identical angular distributions for both γ rays. This is in disagreement with experiment (Ref. 2).